Sheared Plasma Rotation in Partially Stochastic Magnetic Fields

A. Wingen and K. H. Spatschek

Institut für Theoretische Physik, Heinrich-Heine-Universität Düsseldorf, D-40225 Düsseldorf, Germany

(Received 8 October 2008; published 7 May 2009)

It is shown that resonant magnetic perturbations generate sheared flow velocities in magnetized plasmas. Stochastic magnetic fields in incomplete chaos influence the drift motion of electrons and ions differently. Using a fast mapping technique, it is demonstrated that a radial electric field is generated due to the different behavior of passing particles (electrons and ions) in tokamak geometry; magnetic trapping of ions is neglected. Radial profiles of the polodial velocity resulting from the force balance in the presence of a strong toroidal magnetic field are obtained. Scaling laws for plasma losses and the forms of sheared plasma rotation profiles are discussed.

DOI: 10.1103/PhysRevLett.102.185002 PACS numbers: 52.25.Fi, 05.40.−a, 52.25.Gj

Particle and heat transport in stochastic media are central topics of theoretical and experimental research, especially in plasma astrophysics and nuclear fusion. A variety of problems, such as low-energy cosmic ray penetration into the heliosphere, the propagation of galactic cosmic rays in and out of the interstellar magnetic field, turbulent transport in tokamaks, anomalous escape rates of runaways in the atmosphere, and so on, are directly related to charged particle motion in fluctuating fields [1–4]. The interest of plasma physics, especially of nuclear fusion research, in stochastic transport [5–7] recently further increased due to the experimentally realized possibility of generating controlled magnetic fluctuation spectra by external sources. Perturbation coils have been installed in the tokamaks Tore-Supra, TEXTOR, DIII-D, and JET [8,9]. It turned out that the so-called ergodic divertor coils have significant influences on several important plasma phenomena, such as edge localized modes (ELMs) [10], the impurity pinch from a ratchet process [11], and the topology of heat flow patterns [12,13]. The experimental as well as theoretical research on fluctuation-induced transport thereby entered a new stage, with new understanding of basic aspects and auspicious applications. Among the latter certainly is the control of edge plasmas up to the substantial ELM mitigation [14,15] with application to ITER.

In this Letter we discuss the generation of sheared plasma flows by resonant magnetic perturbations (RMPs). Zonal flows are prominent examples of flow generation by nonlinearities in plasmas. In stochastic magnetic fields, built-in ambipolarity of regular fields in tokamaks is destroyed, resulting in a radial electric field and thus sheared flow velocities. Turbulent transport reduction by zonal flows or $E \times B$ shear stabilization in magnetized plasmas are known processes during the self-organization of plasmas far from equilibrium [16,17]. The appearance of transport barriers and the transition to high-confinement modes [7] are fundamental consequences. The interesting point in the present context is that a sheared plasma flow may be generated by controllable magnetic fluctuations as produced by ergodic divertor coils in tokamaks. This should be understood as an amendatory effect to the well-known neoclassical poloidal rotation; the latter is discounted here due to the nonconsideration of magnetically trapped ions and the disregarded collisions. In collisionless plasmas with inhomogeneous magnetic fields, particle orbits deviate from the magnetic field lines due to drifts. The different escape rates of drifting electrons and ions, respectively, from stochastic regions were considered in Refs. [18,19]. Each species was investigated separately. However, because of the different electric charges, space charge induced electric fields $\vec{E} = -\vec{\nabla}\phi$ are generated when both species are simultaneously present. That has not been analyzed so far. In incomplete magnetic chaos electrons may feel, e.g., transport inhibiting cantori while ions do not, and vice versa, depending on the strength of the control parameter (current in the perturbation coils). Thereby the magnitude of the radial electric space charge fields becomes strongly space-dependent. Together with the ambient (toroidal) magnetic field B, a significant $E \times B$ velocity is created. The latter causes a poloidal plasma rotation. For example, in the tokamak TEXTOR without dynamic ergodic divertor (DED), the plasma at the edge rotates in the electron diamagnetic drift (EDD) direction. Here, we shall show that due to the generated space charge fields in the presence of RMPs, the poloidal plasma rotation spins up in the ion diamagnetic drift (IDD) direction and a rotational shear is created. Experimental results support this picture. In addition to toroidal rotation [20,21], a modified poloidal plasma rotation was observed in the presence of magnetic edge perturbations [22].

For a theoretical understanding of the interplay between flows and RMPs we use, for demonstration, the stochastic magnetic fields produced by the DED in TEXTOR. In TEXTOR, the perturbation coils producing RMPs are situated at the high-field (inner) side of the torus. The perturbation current I_0 is alterable. Typical parameters used here are toroidal magnetic field strength $B_0 = 2.2$ T, poloidal plasma beta $\beta_{\mathrm{pol}} \approx 3.92$, plasma center $R_a = 1.75$ m,

 © 2009 The American Physical Society

plasma radius $a = 0.46$ m, temperatures $T_e \approx T_i \approx 10$ keV (as upper limits; we have checked that for temperatures of order 1 keV one gets similar results), and plasma density $n_e \approx n_i \approx 2.8 \times 10^{19}$ m^{-3}. First, we keep the plasma current fixed at $I_p = 390$ kA. The toroidal component A_φ of the magnetic vector potential is being calculated exactly from the current distribution [9]; it is directly proportional to I_0 and, in Fourier representation at a fixed radial position, its maximum value decays with the poloidal mode number m, i.e., $A_\varphi \sim I_0 b^m$, where $b < 1$ is a constant depending on radial position. At a fixed radial position, the mode number of the confining magnetic field varies as $m \sim q \sim I_p^{-1}$, where $q = m/n$ is the safety factor. In other words, for the perturbations the location of resonance with a certain mode number m (note, $n = n_0$ is more or less fixed) varies with the strength of I_p.

The analysis starts from the drift Hamiltonian

$$H = \frac{R}{B_0 R_a}\left(-A_\varphi + \frac{\sigma}{q} mc^2\left[\gamma^2 - 1 - 2\frac{R_a \Omega J_R}{mc^2 R}\right]^{1/2}\right) \quad (1)$$

for each species with mass m and charge q. Here, $\gamma = 1 + (E_{\mathrm{kin}} + q\phi)/mc^2$, Ω is the gyrofrequency, and $J_R \approx c^2\{[0.1(\gamma - 1) + 1]^2 - 1\}/2\Omega^2 R_a^2$. Equation (1) is equivalent to Eq. (32) in Ref. [19], obtained by returning to dimensional (physical) variables using Eqs. (1)–(3), (5), and (26) of the same reference. The formulation ignores magnetically trapped ions and collisions. In case of vanishing perturbations, intact electron drift surfaces approximately coincide with magnetic surfaces while drift surfaces of copassing ($\sigma = +1$) ions are shifted outwards, i.e., to the low-field side, and drift surfaces of counterpassing ($\sigma = -1$) ions are shifted inside. Instead of solving the continuous Hamiltonian equations $dR/d\varphi = R\partial H/\partial z$ and $dz/d\varphi = -R\partial H/\partial R$ for each species, we analyze the electron and ion motion simultaneously by generalizing the fast drift mapping procedure [19] to include self-consistent electric fields. In general, the self-consistency conditions should also take care of Ampere's law in addition to quasineutrality [23]. We neglect this effect here because of the relative smallness of the RMPs. To determine the scalar potential of the ambipolar electric field, the fast mapping technique is combined with an iterative procedure, the Picard iteration. First we pick a random set of equally distributed initial values for electrons *and* ions between the last closed drift surface (LCDS), defined by the plasma radius a and the major radius of the plasma center R_a, and some arbitrary inner boundary (e.g., at a minor radius of 0.1 m). To ensure quasineutrality we choose the same initial numbers of electrons and ions. The numbers of test particles should not be too small to guarantee reliable statistical evaluations. Since we are mainly interested in the electric field at the plasma edge, we spare the calculation of the interior. Thereby we assume that the electric field vanishes in the central plasma; there we have a zero average charge density. The particle energies are drawn from Maxwellian distributions with the electron temperature T_e and the ion temperature T_i, respectively. Next we move the test particles, using the mapping. In the present simulation we assume the particles as thermally distributed with a small drift velocity associated with plasma current. Both the electron as well as the ion ensemble consist of copassing and counterpassing particles with respect to the plasma current. After a reasonable number of iterations, statistical independence from the detailed initial conditions occurs. Different sets of initial conditions within the same set of parameters lead to almost the same results. We make Poincaré plots and determine the surface charge density $\rho(r, \theta)$ in the Poincaré section (r, θ). We renormalize the charge density obtained with the chosen number of test particles (e.g., initially 20 000 electrons and 20 000 ions) to fixed, physically relevant initial particle number densities n_e and n_i, respectively. The independence of the results with respect to the chosen number of test particles has been checked numerically by varying the number of test particles. Then we solve the two-dimensional Poisson equation for the corresponding scalar potential. Note that any field in the toroidal direction is neglected here due to the fast motion of the particles along the field lines inside the torus. In a next iterative step we start again with the same set of initial conditions, but now the scalar potential is included into the mapping. After the same number of iterations we recalculate the charge density and the scalar potential. By continuing this procedure we achieve a stationary solution for the scalar potential, which corresponds to the self-consistent electric field for the chosen parameter configuration. The convergence of the iteration scheme has been checked numerically.

Figure 1 shows the calculated poloidal plasma rotation profiles at the plasma edge for various strengths of magnetic perturbations, realized by different DED perturbation

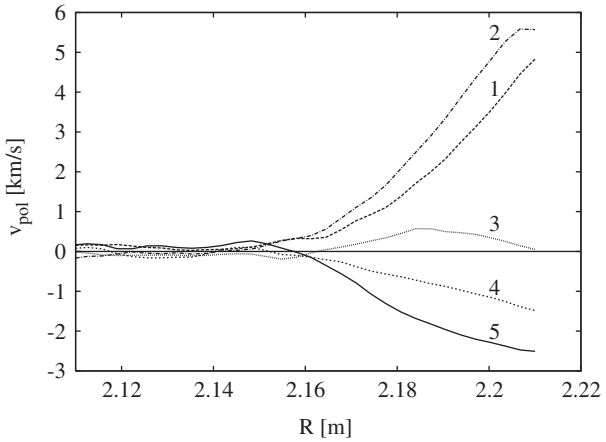

FIG. 1. Poloidal rotation profiles for various DED perturbation currents. Curve 1: Reference state $I_0 = 0$ kA; curve 2: $I_0 = 4$ kA; curve 3: $I_0 = 6.672$ kA; curve 4.: $I_0 = 8$ kA; curve 5: $I_0 = 11$ kA.

currents. The velocity profiles are plotted against the major radius (low-field side to the right). The LCDS is located at a major radius of $R = 2.21$ m. Deep inside the plasma there is almost no radial electric field. About 10 cm inside the LCDS all rotation profiles are almost identical and there is still no poloidal rotation. At about 7 cm inside the LCDS is the onset of the ergodic region for the perturbed case. Now, the detailed behavior is as follows: We start from the reference case 1 without magnetic perturbations ($I_0 = 0$). It shows a continuous increase of the poloidal rotation velocity in the EDD direction (positive poloidal direction) with increasing major radius, up to 5 km/s at the LCDS. At about 5 cm inside the LCDS the poloidal rotation profiles in the presence of stochastic magnetic fields deviate from the reference state, depending on the perturbation current. For small perturbation currents, up to approximately 4 kA, the poloidal rotation velocity is even larger in the EDD direction; see curve 2 in Fig. 1. For bigger perturbations, the poloidal rotation drops to zero and reverses. About $I_0 = 6.672$ kA is the critical perturbation for a zero poloidal rotation at the LCDS; curve 3. For larger perturbations ($I_0 = 8$ kA and $I_0 = 11$ kA are designated by 4 and 5, respectively) the poloidal plasma rotation is in the IDD direction.

The change of the poloidal plasma rotation can be understood from the Poincaré sections for electrons and ions, respectively. For the same number of initial positions the Poincaré sections for electrons show that, within the ergodic region, at $I_0 = 4$ kA the number of intersections of electron drift orbits is significantly larger than in the $I_0 = 6.672$ kA case. This indicates that, although the DED creates already a wide stochastic area for $I_0 = 4$ kA, there is still an almost intact electron drift surface (cantorus) at the position of the electron LCDS. For larger currents the electron drift surface gets more and more destroyed, which leads to a significant increase in electron losses. For the ions, because of their larger masses and thereby smaller velocities, the drift surface at the position of the ion LCDS is already broken at $I_0 = 4$ kA, allowing for a faster loss of ions below $I_0 = 6.672$ kA. Thus, for small perturbations (up to $I_0 \approx 4$ kA) mainly ions are lost to the wall within the perturbed plasma edge, the radial electric field gets more negative, and the poloidal plasma rotation increases in the EDD direction. That effect (at small perturbation currents) depends on temperature; it is more pronounced at large temperatures. When the electron LCDS breaks up, the electron losses increase, and the poloidal rotation drops. At about $I_0 = 6.672$ kA the average radial electric field at the position of the LCDS vanishes, and the poloidal rotation becomes zero. By further increasing the perturbation, the poloidal rotation reverses and increases in the IDD direction. So, when both LCDSs are broken, the electron losses outbalance the ion losses. For large perturbations, the electrons move to the wall much faster than the ions, and a commensurate ambipolar potential appears.

To find the critical perturbation for the breakup of the LCDSs for electrons and ions, respectively, we analyze the escape rates. We start with N_0 test particles (electrons *or* ions) on an unperturbed drift surface, being equally distributed along the whole poloidal angle. Then we turn on the perturbations and iterate until the particles hit the wall, where they are eliminated. The calculation is stopped when 90% of the particles are lost. $N(t)$ is the number of particles in the system at time t. Thereby t corresponds directly to the number of toroidal rotations given by the number of iterations. In open systems, $N(t)/N_0$ is called the escape rate. The escape rate follows a universal kinetic decay law typical for chaotic systems. We make an ansatz in classically diffusive form

$$N(t) = N_0(N_1 + e^{-\lambda t}), \tag{2}$$

where a small offset N_1 resulting from test particles on stable orbits within the ergodic region has been introduced. Figure 2 shows the numerically determined exponent λ for electrons. The decay parameter scales quadratically with the perturbation current in the form $\lambda \sim (I_0 - I_c)^2$. We have $\lambda = 0$ for $I_0 \leq I_c$. Such a law exists for both electrons and ions. Two conclusions can be drawn from this result. First, the escape is diffusive in accordance with the quasilinear prediction of a quadratic dependence on the perturbation [3]. Second, we can extrapolate the value of I_c for electrons from the linear fit in Fig. 2. We find $I_{ce} \approx 3.7$ kA for electrons. The corresponding result for ions is $I_{ci} \approx 2.2$ kA. These findings confirm the interpretation for a qualitative change of the rotation profiles at $I_0 \approx 4$ kA.

We finally varied the plasma current I_p which is inversely proportional to the safety factor q_a at the LCDS. When decreasing the edge safety factor in the perturbed system, the resonances are shifted towards the wall and subsequently are destroyed. Particle escape is directly related to the last resonance at the edge of the ergodic zone. At a certain point when an island chain is destroyed,

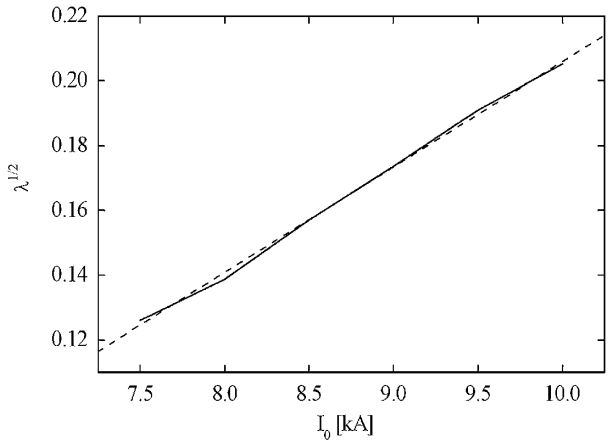

FIG. 2. Square root of the decay parameter λ for electrons dependent on the perturbation current I_0. The dashed line shows a linear fit curve for $\sqrt{\lambda}$.

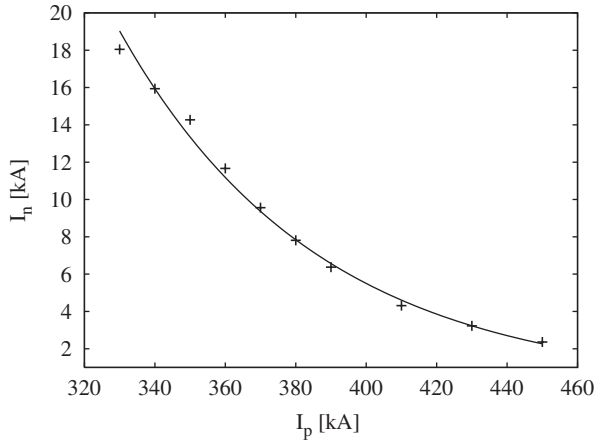

FIG. 3. I_n for zero poloidal rotation velocity versus plasma current I_p. The solid line is the exponential decay fitting curve for the numerically determined crosses.

the next resonance becomes dominant. Previously dominant resonances do not disappear completely. By calculating the poloidal rotation profiles for plasma currents I_p between 330 and 450 kA, we find that, in principle, the poloidal plasma rotations show similar qualitative behaviors as for $I_p = 390$ kA. However, the necessary perturbation current I_n for a zero poloidal rotation velocity at the radial position of the LCDS changes with I_p. Quantitative results are depicted in Fig. 3. For each plasma current the poloidal rotation profile was calculated and the necessary perturbation current I_n for a zero poloidal rotation velocity was determined. The crosses in Fig. 3 mark typical values I_n. We fitted the data by $I_n = Ae^{-\alpha I_p}$; the numerical fitting parameters are $A = 6614.8$ kA and $\alpha = 0.0177$ kA^{-1}. From here we can conclude that the critical perturbations for the breakup of the LCDSs for electrons and ions scale in the same way. Less magnetic perturbations are needed to destroy the LCDS for smaller edge safety factors. This can be understood as follows. Reversal of the flow velocity requires a certain perturbation strength. According to the current and mode number dependencies of the vector potential perturbations, the current for zero poloidal rotation velocity at the LCDS then satisfies $I_n b^{c/I_p} \approx$ const, when $m \approx c/I_p$, $c > 0$ is being used. Thus we find $I_n \sim b^{-c/I_p} \approx Ae^{-\alpha I_p}$ for $b < 1$. The good agreement of the theoretical prediction with the fitting curve in Fig. 3 has been checked numerically.

In summary, we have shown that RMPs strongly influence the electron and ion drift surfaces at the plasma edge. The ambipolar particle dynamics leads to the generation of radial electric fields and a corresponding sheared poloidal plasma rotation.

This research has been performed in cooperation with IEF-4 at FZ Jülich. Discussions with Bernhard Unterberg, Ulrich Samm, and Sadrilla Abdullaev are gratefully acknowledged.

[1] F. Casse, M. Lemoine, and G. Pelletier, Phys. Rev. D **65**, 023002 (2001).
[2] M. Vlad, F. Spineanu, J. H. Misguich, and R. Balescu, Phys. Rev. E **67**, 026406 (2003).
[3] Y. Elskens and D. Escande, *Microscopic Dynamics of Plasmas and Chaos* (IOP, Bristol, 2003).
[4] P. Chuychai, D. Ruffolo, W. H. Matthaeus, and G. Rowlands, Astrophys. J. **633**, L49 (2005).
[5] K. Burrell, Science **281**, 1816 (1998).
[6] Z. Lin, T. Hahm, W. Lee, W. Tang, and R. White, Science **281**, 1835 (1998).
[7] K. Itoh, S.-I. Itoh, and A. Fukuyama, *Transport and Structural Formation in Plasmas* (IOP, Bristol, 1999).
[8] A. Grossman, Plasma Phys. Controlled Fusion **41**, A185 (1999).
[9] K. H. Finken, S. S. Abdullaev, M. Jakubowski, M. Lehnen, A. Nicolai, and K. H. Spatschek, in *The Structure of Magnetic Field in the TEXTOR-DED*, Energy Technology Vol. 45 (Forschungszentrum Jülich, Jülich, 2005).
[10] T. Evans *et al.*, Phys. Rev. Lett. **92**, 235003 (2004).
[11] M. Vlad, F. Spineanu, and S. Benkadda, Phys. Rev. Lett. **96**, 085001 (2006).
[12] M. Jakubowski *et al.*, Phys. Rev. Lett. **96**, 035004 (2006).
[13] A. Wingen, M. Jakubowski, K. H. Spatschek, S. Abdullaev, K. H. Finken, M. Lehnen, and the TEXTOR-team, Phys. Plasmas **14**, 042502 (2007).
[14] M. Z. Tokar, T. E. Evans, A. Gupta, R. Singh, P. Kaw, and R. C. Wolf, Phys. Rev. Lett. **98**, 095001 (2007).
[15] T. E. Evans *et al.*, Nature Phys. **2**, 419 (2006).
[16] H. Biglari, P. Diamond, and P. Terry, Phys. Fluids B **2**, 1 (1990).
[17] T. Hahm and K. Burrell, Phys. Plasmas **2**, 1648 (1995).
[18] S. S. Abdullaev, A. Wingen, and K. H. Spatschek, Phys. Plasmas **13**, 042509 (2006).
[19] A. Wingen, S. Abdullaev, K. H. Finken, M. Jakubowski, and K. H. Spatschek, Nucl. Fusion **46**, 941 (2006).
[20] K. Finken *et al.*, Phys. Rev. Lett. **94**, 015003 (2005).
[21] A. Garofalo, K. Burrell, J. DeBoo, J. deGrassie, G. Jackson, M. Lanctot, H. Reimerdes, M. Schaffer, W. Solomon, and E. Strait, Phys. Rev. Lett. **101**, 195005 (2008).
[22] B. Unterberg *et al.*, J. Nucl. Mater. **363–365**, 698 (2007).
[23] P. Terry, P. Diamond, and T. T. S. Hahm, Phys. Rev. Lett. **57**, 1899 (1986).